

Plasma Degradation of Dibromophenols and Interpretation by Molecular Orbital Theory^{*)}

Tetsuya AKITSU^{1,3)}, Shin-Ichiro KOJIMA²⁾, Keiko KATAYAMA-HIRAYAMA¹⁾, Hiroki KURODA³⁾ and Hiroshi OKAWA³⁾

¹⁾University of Yamanashi, 4 Takeda, Kofu, Yamanashi 400-8511, Japan

²⁾Kyushu University, Fukuoka, Fukuoka 812-8581, Japan

³⁾Happy Science University, 4427-1 Hitotsumatsu-Hei, Chosei, Chiba 299-4325, Japan

(Received 2 January 2019 / Accepted 17 June 2019)

Dielectric barrier discharge was operated in the liquid-gas boundary and applied to the degradation of Dibromophenol (DBP). The brominated aromatic compound show acute toxicity to aqueous living and, occasionally, carcinogenic and hormone-disruptive effect for human. The plasma degradation provides the advanced oxidation process by charged species, anion as well as neutral radicals. Plasma-degradation with the anion-exchange successfully worked and the controlled the production of BrO_3^- by NO_3^- . Interpretation of the observed difference in the resistance is interpreted using the Molecular Orbital Theory.

© 2019 The Japan Society of Plasma Science and Nuclear Fusion Research

Keywords: plasma electrolysis, aromatic compound, advanced oxidation, molecular orbital theory

DOI: 10.1585/pfr.14.3401132

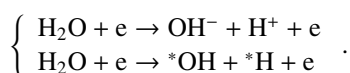
1. Introduction

Increasing amount of aromatic compounds, with multi benzene rings is produced as flame-retardant plastic materials. 2, 6-Dibromophenol (2, 6-DBP) is detected as a degradation product of Tetrabromobisphenol-A (TBBP-A) [1,2]. The environmental toxicity is presented by World Health Organization (WHO) [3]. Concern of the animal carcinogenicity is expressed for a product in the oxidative degradation: BrO_3^- , by the International Agency for Research on Cancer (IARC) classification Group 2B [4]. Degradation of 2, 6-DBP have been studied using a dielectric barrier discharge in the gas-liquid boundary [5]. In this work, we aim at the confirmation of the reproducibility at lower discharge power, and experimental comparison of DBPs: 2, 4-DBP. Degradation at a higher concentration of DBP solution and a short-cut of the degradation using an anion-exchange polymer have been studied.

2. Materials and Methods

Lukes *et al.* [6] reported the measurement of $^*\text{OH}$ radical production and O_3 decomposition in the presence of N_2 molecules in humid air, through the following reactions.

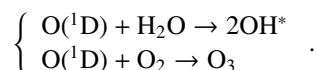
Dissociation and ionization generating OH^- anion and radicals



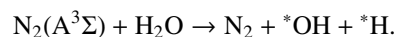
author's e-mail: akitsu@yamanashi.ac.jp

^{*)} This article is based on the presentation at the 27th International Toki Conference (ITC27) & the 13th Asia Pacific Plasma Theory Conference (APPTC2018).

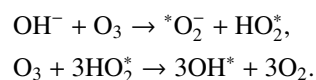
Reactions including excited oxygens



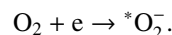
Reactions including metastable state of nitrogen molecules



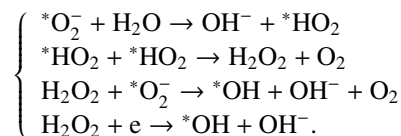
Inhibition of O_3 production and enhancement of OH^* formation:



Production of superoxide: Oxygen molecule is the primary acceptor of electrons and forms $^*\text{O}_2^-$



Production of hydroxyl radicals:



Dibromophenol + $\{^*\text{OH} + \text{OH}^-\}$

→ Produced system.

Hydroxyl radical and anion are produced in the dissociation of hydrogen peroxide by the electron collision in the gas discharge. In the reactions, in air with humidity, one of the merits is the suppression of ozone generation. Ozone quench is important for the suppression of BrO_3^- . The suppression of BrO_3^- is realized by NO_3^- in the advanced oxidation.

Nitrogen reactions including the ozone quench generating the excited state of nitrogen and NO_x

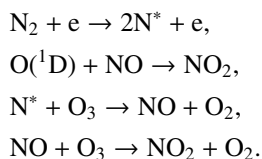


Figure 1 shows the experimental layout. The apparatus consists of a quartz tube 3.0 mm in outer diameter, 1.4 mm in inner diameter and W-Re electrode inserted coaxially. This part is submerged in the DBP water solution in a test vial, 100 mL. Discharge is excited with a quasi-sinusoidal high voltage generated by a fly-back transformer oscillator, at 16.94 kHz, 7.68 to 7.84 kV. Figure 1 (b) shows the High voltage is supplied to a W-Re wire inserted along the center. Discharge current was measured with a current probe and pre-amplifier TCP312 and TCPA300. High-side terminal voltage was measured with P-3000 high voltage probe. Discharge power was estimated by integrating the multiplied waveform and digitized Q versus V Lissajous figure. The electronic charge Q was measured as the voltage-drop across a ceramic capacitor, $C_r = 4200$ pF connected to the outer electrode surrounding the vial.

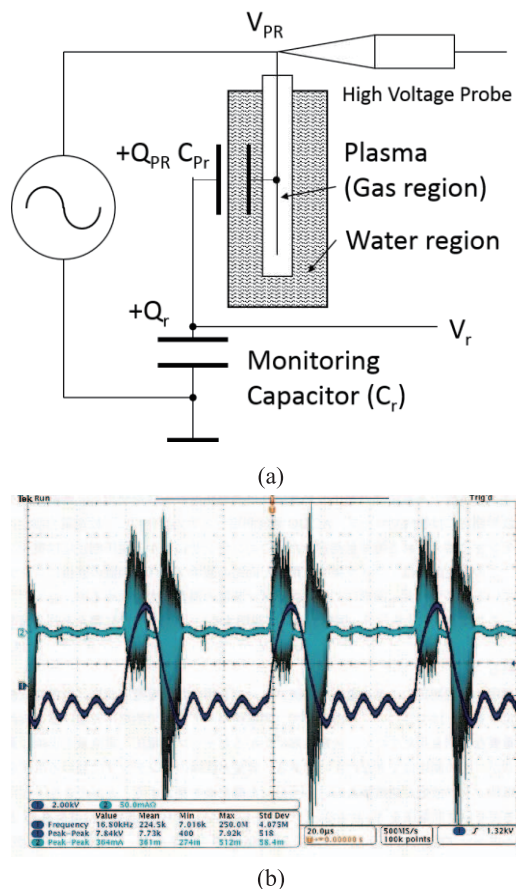


Fig. 1 The dielectric barrier electrode and measurement plasma reactor; (a) Experimental layout; (b) voltage (lower) and current (upper trace) waveform. Vertical unit: 2 kV/div. 50 mA/div. and horizontal unit: 20 μs/div.

In the experiment, DBP sample was solved in NaOH solution, and diluted with pure-water. The concentration was measured at 20 mg/L. After plasma-injection, the concentration of the solution of DBP was measured by the high-performance liquid chromatograph (HPLC). The total organic carbon (TOC) was measure as the amount of CO_2 from the incinerated organic materials. The concentration of Br^- and BrO_3^- was measured by the ion-chromatography. The concentration of the DBPs were measured by HPLC, L-6000 equipped with UV detector, L-4200 (Hitachi Co., Japan) with column X-bridge 4.6, 250 mm (Waters, Japan).

TOC measurement was carried out by TOC-LCSH/CSN and auto sampler, ASI-L, (Shimadzu Co., Japan) Ion chromatography for the anion ICS-1100 (Dionex), with column IonPac AS22 (Dionex), and guard column, IonPac, AG22 (Dionex) installed with the electro-conductivity detector. The reproducibility of the time elapsed measurement and the experiment with high density samples was examined by HPLC Prominence-I LC-2030 Plus (Shimadzu Co., Japan) installed with UV-detector and a reverse mode column: Xbridge C-18, 5 μm.

3. Experimental Results

Figure 2 shows the time-evolution of 2, 6-DBP concentration and TOC as a measure of remaining organic compounds. In Fig. 2 (a), oxygen and air discharge case, one can find that the bromine detachment is completed in 20 minutes. The decomposition in nitrogen (green-diamond) and Ar (blue-triangle symbols) discharge are inefficient compared with the oxidative media.

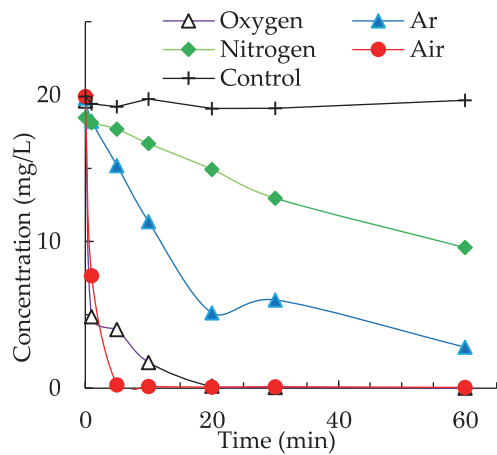
Decrease in the TOC in the oxygen discharge is almost 100%. Figure 3 shows the result of the ion-chromatography: Br^- , and BrO_3^- . NO_3^- was measured in the air discharge. In the oxygen discharge, the increase in the concentration of Br^- anion is observed initially. Then, turned to decrease. This change indicates the production of BrO_3^- by oxidation. In the air-discharge, 40% of the initial TOC is remaining, but the suppression of BrO_3^- production was observed. This difference is attributed to the increase in NO_3^- density. The power estimated with the Q versus V Lissajous is summarized in Table 1.

Next object is the comparison of DBPs structure and the operation at lower discharge power < 6 W. Figure 4 shows the degradation of 2, 4-DBP and 2, 6-DBP, in the initial 20 minutes.

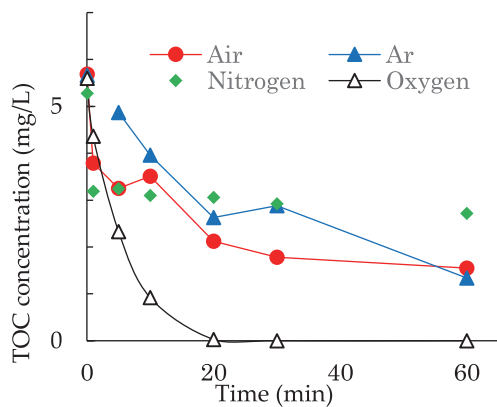
The power estimated with the Q versus V Lissajous is summarized in Table 2, at low discharge power < 6 W.

In Figs. 4 (b) and (c), our small finding is the bromine detachment in shorter time in the case of 2, 6-DBP.

In the industrial bi-product, hazardous concentration of DBP may be observed. Let's say 10 times the observed case. Table 3 shows the result of the combination of the plasma degradation and the anion exchange using gel-type tri-methyl ammonium polymer, after the air-discharge



(a)



(b)

Fig. 2 Comparison of the degradation of 2, 6-DBP by multi-gas plasma; (a) Concentration of 2, 6-DBP. Black-cross symbol indicate the control in a case air bubbling; (b) TOC.

Table 1 Discharge power.

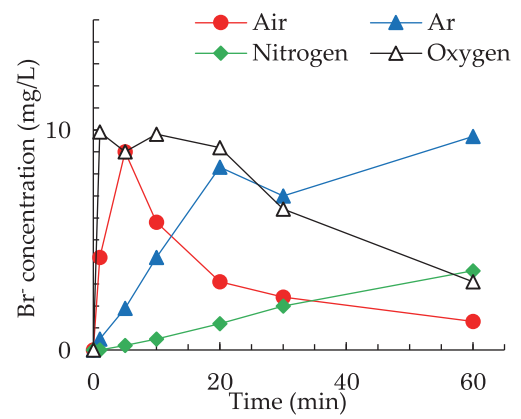
Gas	Energy (mJ/s)	Frequency (kHz)	Power (W)
Air	0.608	16.88	10.26
Ar	0.293	16.69	4.89
N ₂	0.410	16.94	6.94
O ₂	0.749	16.91	12.67

Table 2 Discharge power.

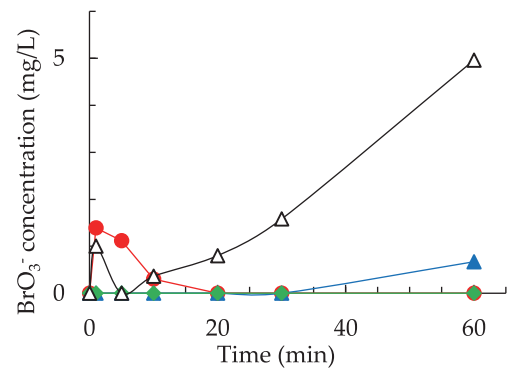
Gas	Energy (mJ/s)	Frequency (kHz)	Power (W)
Air	0.363	16.89	6.13
Ar	0.224	16.99	3.81
N ₂	0.314	16.99	5.33
O ₂	0.354	16.92	5.99

degradation in 10 minutes, at discharge power < 13 W.

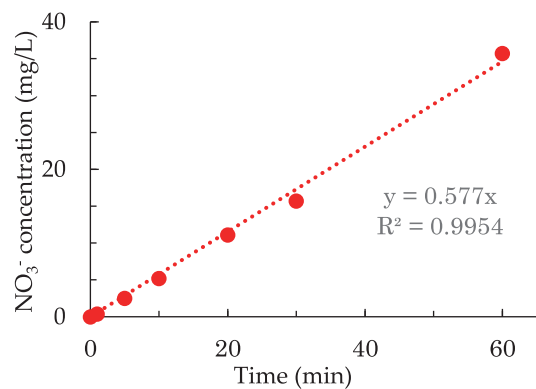
Using the combination of plasma and anion exchange, high density sample can be degraded to 25 % of the initial



(a)



(b)



(c)

Fig. 3 Concentration of anion; (a) Br⁻; (b) BrO₃⁻; (c) NO₃⁻ in the air- discharge case. Dotted line: Linear regression.

Table 3 Combined process of plasma-degradation and anion exchange.

	Control		Air plasma	
	No exchange	exchange	No exchange	exchange
Anion exchange	No	exchange	No	exchange
Color	No	No	Yellow	No
pH.	10.8	9.3	7.5	6.8
Concentration* (mg/L)	200	—	90.3	45.9

*2, 4- DBP

concentration successfully. Thus, a short cut of the degradation have been achieved. Figure 5 shows poly-styrene base anion exchange polymer, capable to exchange Br⁻

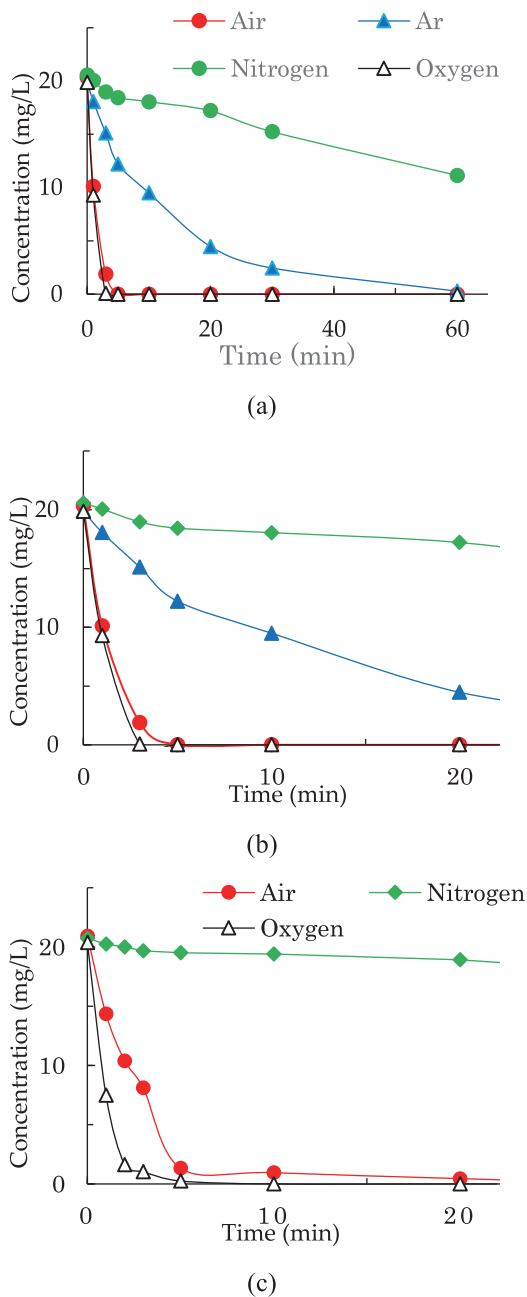


Fig. 4 Experimental comparison of the concentration of DBPs: (a) 2, 6-DBP, (b) 2, 6-DBP initial phase, and (c) 2, 4-DBP.

and NO_3^- anion with OH^- anion.

4. Discussion

4.1 Interpretation by frontier electron density calculation

The replacement reaction of Br^- and OH^- is determined by the energy difference in the starting system, $\text{DBP} + \text{OH}^-$. Consequently, the reversed reaction in the produced system, bromophenol - $\text{OH} + \text{Br}^-$ (in NaBr). Hydroxyl radical and anion are excited in the gas region. The excited state of hydroxyl radicals is singly occupied molec-

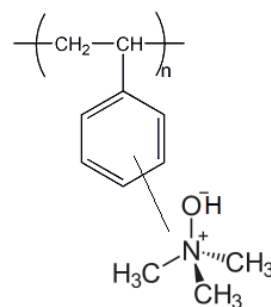


Fig. 5 Gel-type poly-styrene base, tri-methyl ammonium anion exchange polymer. (Sanei Chemistry, Japan).

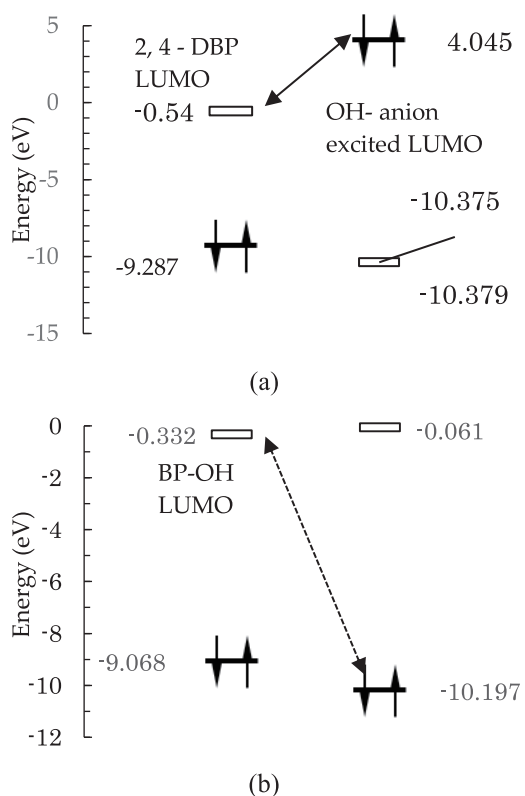


Fig. 6 LUMO and HOMO energy diagram for the Nucleophilic reaction; (a) Starting system, 2, 4-DBP + OH^- ; (b) Produced system, bromophenol - $\text{OH} + \text{Br}^-$ (in NaBr); LUMO energy is -0.332 eV and HOMO -10.197 eV. Empty line symbol indicates LUMO and line with two spins indicates HOMO state.

ular orbital (SOMO) and directed to the electrophilic reaction. Figure 6 shows the energy diagram of the excited state of hydroxyl anion and DBP. The lowest unoccupied molecular orbital, LUMO energy of the starting system, 2, 4-DBP is -0.54 eV and excited energy of OH^- is 4.045 eV. Difference between the highest occupied molecular orbital, HOMO and LUMO energy gives the activation energy, 4.585 eV. LUMO energy of the produced system 1, 2 - OH -4-bromophenol is -0.332 eV and HOMO energy of Br^- is -10.197 eV. This calculation indicates the reaction

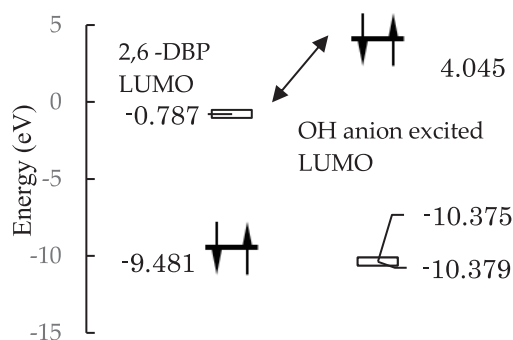
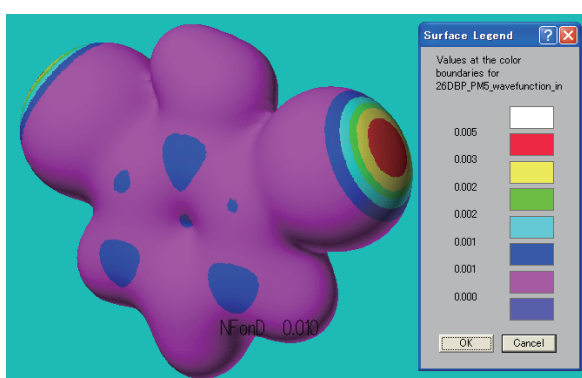
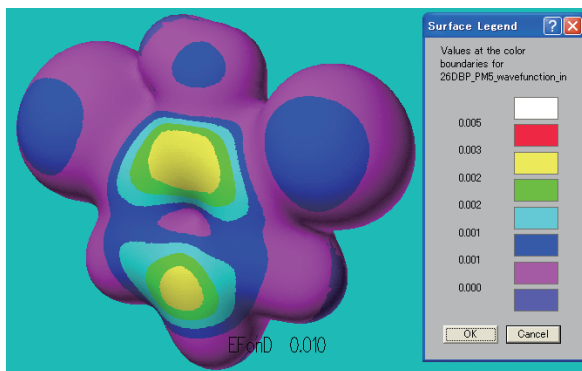


Fig. 7 LUMO and HOMO energy diagram for the Nucleophilic reaction; Starting system, 2, 6 - DBP + OH⁻; Empty line symbol indicates LUMO and line with two spins indicates HOMO state.



(a)



(b)

Fig. 8 Iso-surface of 2, 6 - DBP; (a) the nucleophilic susceptibility, (b) electrophilic susceptibility reaction frontier electron density.

proceeds in the forward direction, while supplies of OH^{*} radical and excited OH⁻ anion lasts. Figure 7 shows the energy diagram of the starting system of 2, 6 - DBP+OH⁻. LUMO energy is slightly lower.

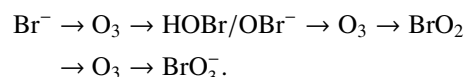
Figure 8 shows iso-surface of the nucleophilic and electrophilic reaction frontier electron density of 2, 6 - DBP. Excited hydroxyl anion is directed to the nucleophilic reaction localized around Br atoms, whereas the reaction with hydroxyl radical is targeted to the electrophilic reac-

tion region localized around the benzene ring.

The frontier electron density was calculated by Biomedical CAChe (Fujitsu, Japan) [7, 8].

4.2 Interpretation of the control of BrO₃⁻ anion

From the experimental result, the highest concentration of BrO₃⁻ is found in the case of the oxygen-discharge. Logically, in the air-discharge contains suggests that BrO₃⁻ is controlled by NO₃⁻. A proposal is made by von Gunten that BrO₃⁻ is produced by the cascade oxidation in the advanced oxidation by oxygen plasma or ozone injection [9–11]. This process is considered as in the following reaction.



Concerning the blocking of BrO₃⁻ in the air plasma, a proposal of the following reaction is made by Parrino *et al.* [12]



Air plasma produces NO₃⁻ anions, and H⁺ is the counter part of OH⁻. The accumulation of this anion lowers the pH. of the system and contributes to the decreases in the concentration of OH⁻. Nevertheless, the reactant is supplied from the gas-region independently, and NO₃⁻ can contribute to the blocking of the production of undesirable byproduct BrO₃⁻.

5. Conclusion

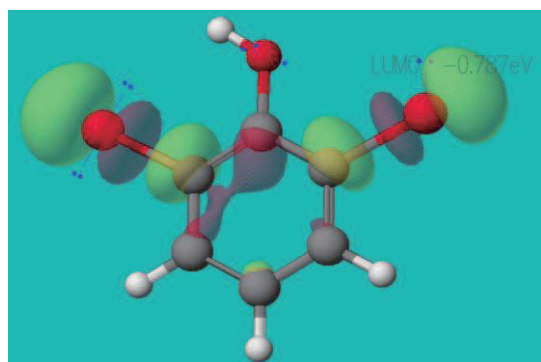
Plasma degradation of dibromophenols was studied using a compact dielectric barrier discharge in a quartz tube, dielectric barrier discharge at the gas-liquid boundary. As the dielectric barrier discharge can be operated at low electric power, this method is a feasible solution for the nature remediation. Experimental comparison of working gas revealed the control of hazardous bi-product BrO₃⁻ was realized by the accumulation of nitric anion in air-discharge. The degradation of Br system was interpreted by the Molecular Orbital Theory. The LUMO energy level of DBP is lower than the excited energy level of the active component, OH⁻. this result suggests that the electrochemical degradation by the plasma satisfies the requirement for the environmental pollution by the brominated aromatic compounds. The direction of the forward reaction was explained by the energy-difference between the starting system and the produced system.

Acknowledgement

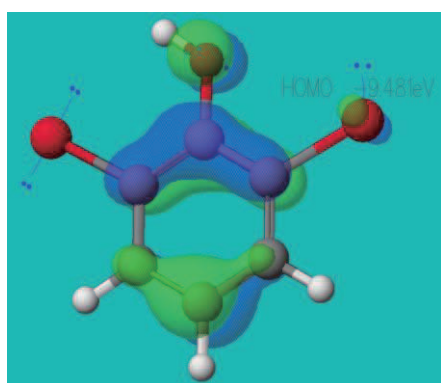
This research received a fund from Future Science Institute, Tokyo, Japan. The authors express their gratitude to Mr. Kento Nakai and Mr. Kenya Yabu for their collaboration.

Appendix A

Figure A shows 3-D LUMO/HOMO model of 2, 6-DBP.



(a)

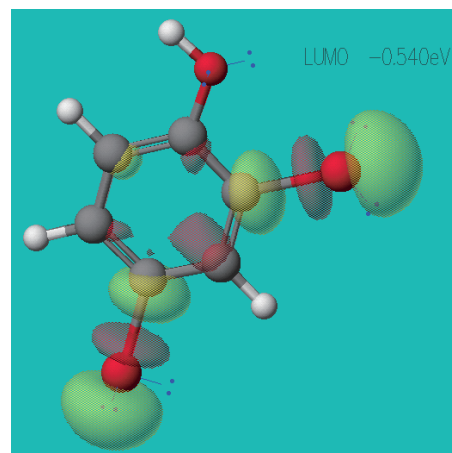


(b)

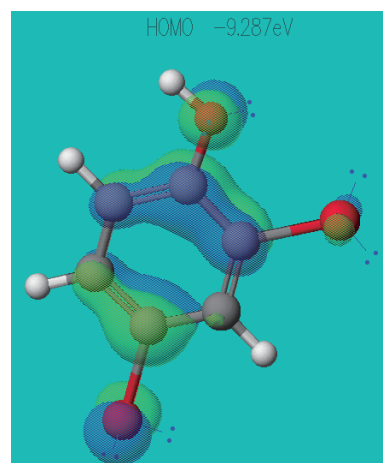
Fig. A 3-D LUMO / HOMO model of 2, 6-DBP. (a) LUMO surface, -0.737 eV; (b) HOMO surface, -9.481 eV.

Appendix B

Figure B shows 3-D LUMO / HOMO model of 2, 4-DBP.



(a)



(b)

Fig. B 3-D LUMO / HOMO model of 2, 4-DBP (a) LUMO surface -0.540 eV, (b) HOMO surface -9.287 eV.

- [1] WHO (World Health Organization) (1995) In: Van Esch GJ, ed., "Tetrabromobisphenol A and Derivatives. Geneva: WHO International Programme on Chemical Safety", Environmental Health Criteria **172**, 25 (1995).
- [2] K. Katayama-Hirayama, A. Suzuki, S. Mukaiyama, K. Hirayama and T. Akitsu, Sustainable Environment Research **20**(4), 221 (2010).
- [3] K. Katayama-Hirayama, N. Toda, A. Tauchi, A. Fujioka, T. Akitsu, H. Kaneko and K. Hirayama, J. Environ. Sci. **26**, 1284 (2014). [http://DOI.ORG/10.1016/S1001-0742\(13\)60600-2](http://DOI.ORG/10.1016/S1001-0742(13)60600-2)
- [4] IARC section 172.730 Potassium Bromate. <https://www.accessdata.fda.gov/scripts/cdrh/cfdocs/cfcfr/CFRSe arch.cfm?fr=172.730>
- [5] S. Kojima, K. Katayama-Hirayama and T. Akitsu, World J. Eng. Technol. **4**, 423 (2016). <http://DOI.ORG/10.4236/wjet.2016.43042>
- [6] P. Lukes and B.R. Locke, Ind. Eng. Chem. Res. **44**(9), 2921 (2005). <https://DOI.ORG/10.1021/ie0491342>
- [7] Biomedical CAChe 6.0 Users Guide (2003), Fujitsu.
- [8] K. Somekawa, *Molecular Orbital Calculation of Organic Molecules and The Applications (MOCOM)* (Kyushu University Press, 2013) ISBN978-4-7985-0089-8.
- [9] U. Von Gunten, Water Res. **37**(7), 1443 (2003). PMID: 12600374.
- [10] U. Von Gunten, Water Res. **37**(7), 1469 (2003). PMID: 12600375.
- [11] U. Von Gunten and J. Holgne, Environ. Sci. Technol. **28**(7), 1234 (1994). <http://DOI.ORG/10.1021/es00056a009>
- [12] F. Parrino, G. Camera - Roda, V. Loddo, V. Augugliaro and L. Palmisano, Appl. Catal. B Environmental **178**, 37 (2013). <http://DOI.ORG/10.1016/j.apcatb.2014.10.081>